

# A Testable Theory for High-Tc Superconductivity in Cuprates

E. C. Marino\*

*Instituto de Física, Universidade Federal do Rio de Janeiro,  
C.P. 68528, Rio de Janeiro, RJ, 21941-972, Brazil.*

(Dated: October 20, 2022)

A number of theories for the superconductivity in cuprates, have been proposed in the more than 30 years that have elapsed since its discovery. A common feature of these theories is the small number, or even the absence, of quantitative predictions that could be compared to a vast number of experimental data, which are, conversely, available. Such theories are, consequently non-testable. We describe the foundations and a number of applications of a theory describing High-Tc Superconductivity in cuprates, which we proposed recently, that besides being testable, has proven to meet successfully the tests to which it has been submitted so far.

## CONTENTS

- 1 Introduction
- 2 The Model
- 3 Phase Diagram
- 4 Resistivity
- 5 Pressure Effects
- 6 Conclusion

## 1 INTRODUCTION

After more than three decades of the discovery of superconductivity in cuprates, different theories have been proposed to explain the underlying mechanism responsible for this phenomenon. Almost all of them, however, failed in providing quantitative predictions that could be compared to the large amount of existing experimental data. Conversely, in a series of recent publications, [1–4] we have proposed a theory for High-Tc superconductivity in cuprates, which does not suffer from this shortcoming. Indeed, our theory makes several quantitative predictions, based on analytic expressions, for the outcome of measurements of physical observables in cuprates. Such observables include: the critical SC transition temperature as a function of doping,  $T_c(x)$ , the pseudogap transition temperature as a function of doping,  $T^*(x)$ , the pressure dependence of the optimal SC transition temperature  $T_{max}(P)$ , the dependence of the optimal SC transition temperature on the number of  $CuO_2$  layers,  $T_{max}(N)$ , the resistivity as a function of temperature and magnetic field ( $\rho(T)$  and  $\rho(H)$ ) in the normal (non SC) phases and the spectral weight, among other observable quantities. All of these compare quite well with the experimental data for several cuprate materials [1–4] including LSCO, YBCO, Hg1201, Hg1212, Hg1223, Bi2201, Bi2212, Bi2213. Our theory is, therefore, testable and thus fulfills one of the first prerequisites of any acceptable theory and, beyond that, it has proven to pass all the tests to which it has been sub-

mitted so far.

The theory we propose is derived from the Spin-Fermion-Hubbard (SFH) Model [6–8], and its Hamiltonian is obtained from the SFH, by performing two standard operations, [1] namely: a) tracing out the localized spins degrees of freedom; and b) making a second order perturbation theory on  $t/U$ , the ratio of the hopping to the Hubbard parameters.

An additional key ingredient of our theory is the fact that a dimerization occurs in the bipartite oxygen square lattice. Such dimerized configuration is energetically more favorable and is directly responsible for the onset of a superconducting state in the cuprates [4]. Such state has resonating spin zero dimers, similarly to the RVB state [9–11]. In our case, however, differently from the RVB state the resonating dimers are themselves Cooper pairs formed by two holes with opposite spins and belonging to different nearest neighbor sub-lattices [4].

We have successfully applied our theory in the explanation of the results of several experiments performed in the cuprates [1–4], hence our claim that our theory is not only testable: most importantly, it has passed the several tests to which it has been submitted so far.

## 2 THE MODEL

### 2.1 The Starting Hamiltonian

The first step before writing a model hamiltonian for this system consists in the realization that the  $CuO_2$  planes, which are the stage upon which the physics of cuprates unfold, contain three intertwined square lattices: the one containing the localized  $Cu$  spins, and the bi-partite square lattice containing the itinerant spin 1/2 oxygen holes, belonging to  $p_x$  and  $p_y$  orbitals that alternatively hybridize with the  $Cu^{++} d_{x^2-y^2}$  orbitals.

The  $A, B$  oxygen sub-lattices are located, respectively,

at  $(\mathbf{R}, \mathbf{R} + \mathbf{d}_i)$ , where

$$\begin{aligned} \mathbf{d}_1 &= \frac{1}{2}[\mathbf{X} - \mathbf{Y}] ; \quad \mathbf{d}_2 = \frac{1}{2}[\mathbf{X} + \mathbf{Y}] \\ \mathbf{d}_3 &= \frac{1}{2}[-\mathbf{X} + \mathbf{Y}] ; \quad \mathbf{d}_4 = \frac{1}{2}[-\mathbf{X} - \mathbf{Y}], \end{aligned} \quad (1)$$

where  $\mathbf{X} = a\hat{x}$  and  $\mathbf{Y} = a\hat{y}$  are primitive vectors of the oxygen lattices (see [1]).

In order to derive our theory for the high- $T_c$  superconductivity (SC) in cuprates, we start from the the Spin-Fermion-Hubbard (SFH) Hamiltonian, which comprises the four terms below [1, 4, 5]: the hopping term, the AF Heisenberg term, the Kondo-like term and the Hubbard term, namely

$$H_{SFH} = H_0 + H_{AF} + H_K + H_U$$

$$H_0 = -t_p \sum_{\mathbf{R}, \mathbf{d}_i} \sum_{\sigma} \psi_{A,\sigma}^{\dagger}(\mathbf{R}) \psi_{B,\sigma}(\mathbf{R} + \mathbf{d}_i) + hc$$

$$H_{AF} = J_{AF} \sum_{\langle IJ \rangle} \mathbf{S}_I \cdot \mathbf{S}_J$$

$$H_K = J_K \sum_I \mathbf{S}_I \cdot \left[ \sum_{\mathbf{R} \in I} \eta_A \eta_C \mathcal{S}_A + \sum_{\mathbf{R} + \mathbf{d} \in I} \eta_B \eta'_C \mathcal{S}_B \right]$$

$$H_U = U_p \sum_{\mathbf{R}} n_{\uparrow}^A n_{\downarrow}^A + U_p \sum_{\mathbf{R} + \mathbf{d}} n_{\uparrow}^B n_{\downarrow}^B \quad (2)$$

where  $\psi_A^{\dagger}(\mathbf{R})$ ,  $\psi_B^{\dagger}(\mathbf{R} + \mathbf{d})$  are the hole creation operators on sites  $\mathbf{R}$  and  $\mathbf{R} + \mathbf{d}$ , respectively, of the  $A, B$  oxygen sub-lattices and  $\mathbf{S}_I$  are the spin operators of the localized  $Cu^{++}$  ions.

In the expression above,

$$\mathcal{S}_{A,B} = \frac{1}{2} \psi_{(A,B)\alpha}^{\dagger} \vec{\sigma}_{\alpha\beta} \psi_{(A,B)\beta} \quad (3)$$

is the spin operator of the holes belonging to the  $p_x, p_y$  oxygen orbitals, associated, respectively, to the  $A$  and  $B$  sub-lattices. The sign factors  $\eta_A, \eta_B, \eta_C, \eta'_C = \pm 1$  come from the  $pd$ -hybridization integrals involving the overlap of  $p$  and  $d$  atomic orbitals. We are going to consider the orbital array depicted in Fig. 1, for which the product  $\eta_A \eta_B \eta_C \eta'_C$  for nearest neighbors  $A, B$  is always equal to  $-1$ .

We derive our effective Hamiltonian for the cuprates by performing two standard familiar operations on Hamiltonian (2). These are: a) tracing out the localized spins  $\mathbf{S}_I$ , in  $H_{AF} + H_K$  and b) making a perturbative expansion on  $H_U + H_0$ .

## 2.2 Tracing the Localized Spins

We start by tracing out the localized spins [5].

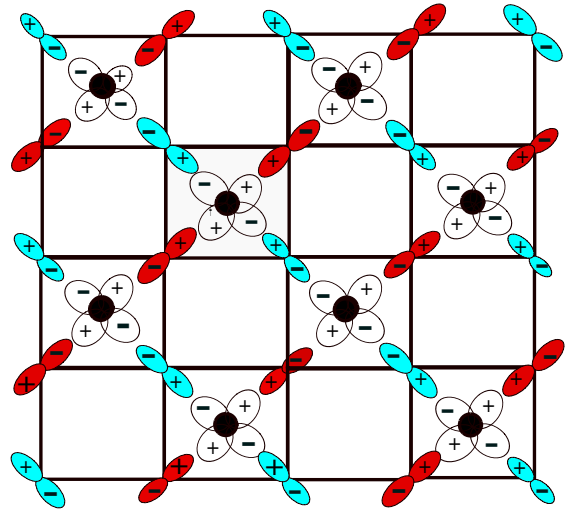


FIG. 1: The  $CuO_2$  planar lattice with sub-lattices  $A$  and  $B$  represented in red and cyan, respectively. This configuration leads the magnetic interaction between localized and itinerant spins to an effective hole-attractive interaction for all nearest neighbor holes and is responsible for the superconductivity in cuprates.

We have the partition function given by

$$Z = \text{Tr}_{\psi} \text{Tr}_{\mathbf{S}_I} e^{-\beta[H_0[\psi] + H_U[\psi] + H[\mathbf{S}_I, \psi]]} \quad (4)$$

By using a base of coherent spin states,  $\{|\mathbf{N}\rangle\}$ , labeled by the unit vector  $\mathbf{N}$  and having the property

$$\langle \mathbf{N} | \mathbf{S}_I | \mathbf{N} \rangle = s \mathbf{N}_I \quad (5)$$

( $s = 1/2$  is the spin quantum number), we can express the trace over the localized spins  $\mathbf{S}_I$  as a functional integral over the classical vector field  $\mathbf{N}$  of unit length (see, for instance [1]) from which, we have [5]

$$\text{Tr}_{\mathbf{S}_I} e^{-\beta H[\mathbf{S}_I, \psi]} = \int D\mathbf{N} \delta(|\mathbf{N}|^2 - 1) e^{-\beta H[s\mathbf{N}_I, \psi]} \quad (6)$$

We now decompose  $\mathbf{N}$  in terms of antiferromagnetic and ferromagnetic components, denoted, respectively, by  $\mathbf{n}$  and  $\mathbf{L}$ . We then write, in terms of the lattice parameter  $a$ :

$$\mathbf{N}_I = (-1)^I \mathbf{n}_I \sqrt{1 - a^4 \mathbf{L}^2} + a^2 \mathbf{L}_I \quad (7)$$

such that  $|\mathbf{N}|^2 = |\mathbf{n}|^2 = 1$  and  $\mathbf{L} \cdot \mathbf{n} = 0$ .

We can re-write the trace over  $\mathbf{S}_I$  as a double functional integral on  $\mathbf{n}$  and  $\mathbf{L}$  [1]:

$$\text{Tr}_{\mathbf{S}_I} = \int D\mathbf{n} D\mathbf{L} \delta(|\mathbf{n}|^2 - 1) \quad (8)$$

Then, inserting (7) in (6) and expanding in  $a$ , we obtain

$$\begin{aligned} \text{Tr}_{\mathbf{S}_I} e^{-\beta H[\mathbf{S}_I, \psi]} &= \int D\mathbf{n} D\mathbf{L} \delta(|\mathbf{n}|^2 - 1) \\ \exp \left\{ -\frac{1}{2} \int d^2r \int_0^\beta d\tau [J_{AF} s^2 \nabla_i \mathbf{n} \cdot \nabla_i \mathbf{n} \right. \\ &+ 4J_{AF} s^2 a^2 |\mathbf{L}|^2 \\ &\left. + \mathbf{L} \cdot \left[ J_K [\eta_A \eta_C \mathcal{S}_A + \eta_B \eta'_C \mathcal{S}_B] - i s \mathbf{n} \times \frac{\partial \mathbf{n}}{\partial \tau} \right] \right\} \end{aligned} \quad (9)$$

$$\begin{aligned} \text{Tr}_{\mathbf{S}_I} e^{-\beta H[\mathbf{S}_I, \psi]} &= \int D\mathbf{n} \delta(|\mathbf{n}|^2 - 1) \times \\ \exp \left\{ - \int d^2r \int_0^\beta d\tau \frac{\rho_s}{2} \left[ \nabla_i \mathbf{n} \cdot \nabla_i \mathbf{n} + \frac{1}{c^2} \partial_\tau \mathbf{n} \cdot \partial_\tau \mathbf{n} \right] \right. \\ &\left. + \frac{J_K^2}{8J_{AF} a^2} \left[ \sum_{\mathbf{R} \in I} \eta_A \eta_C \mathcal{S}_A + \sum_{\mathbf{R} + \mathbf{d} \in I} \eta_B \eta'_C \mathcal{S}_B \right] \cdot \left[ \sum_{\mathbf{R} \in I} \eta_A \eta_C \mathcal{S}_A + \sum_{\mathbf{R} + \mathbf{d} \in I} \eta_B \eta'_C \mathcal{S}_B \right] \right\} \end{aligned} \quad (10)$$

where  $\rho_s = \frac{J_{AF}}{4}$  is the spin stiffness and  $c = J_{AF} a$  is the spin-waves velocity.

Using the fact that the continuum limit involves the replacement  $a^2 \sum_{\mathbf{R}} \leftrightarrow \int d^2r$ , we conclude that

$$\text{Tr}_{\mathbf{S}_I} e^{-\beta [H_{AF}[\mathbf{S}_I] + H_K[\mathbf{S}_I, \psi]]} = Z_{NL\sigma M} e^{-\beta H_1[\psi]} = Z_{NL\sigma M} \exp \left\{ - \int_0^\beta d\tau \sum_{\mathbf{R}, \mathbf{R} + \mathbf{d}} \left[ \frac{J_K^2}{8J_{AF}} [\eta_A \eta_C \mathcal{S}_A + \eta_B \eta'_C \mathcal{S}_B]^2 \right] \right\} \quad (11)$$

where  $Z_{NL\sigma M}$  is the partition function of the Nonlinear Sigma Model ( see, for instance [5]).

Inserting the expressions for  $\mathcal{S}_A$  and  $\mathcal{S}_B$  in (9), we obtain, up to a constant,

$$\begin{aligned} H_1[\psi] &= \\ \frac{J_K^2}{8J_{AF}} \eta_A \eta_B \eta_C \eta'_C &\sum_{\mathbf{R}, \mathbf{R} + \mathbf{d}_i} \left[ \psi_{A\uparrow}^\dagger(\mathbf{R}) \psi_{B\downarrow}^\dagger(\mathbf{R} + \mathbf{d}_i) + \psi_{A\downarrow}^\dagger(\mathbf{R}) \psi_{B\uparrow}^\dagger(\mathbf{R} + \mathbf{d}_i) \right] \left[ \psi_{B\downarrow}(\mathbf{R} + \mathbf{d}_i) \psi_{A\uparrow}(\mathbf{R}) + \psi_{B\uparrow}(\mathbf{R} + \mathbf{d}_i) \psi_{A\downarrow}(\mathbf{R}) \right] \end{aligned} \quad (12)$$

From Fig. 1 we see that

$$\eta_A \eta_C \eta_B \eta'_C = -1. \quad (13)$$

For this reason, the above interaction is always attractive between nearest neighbor holes, which belong to different sub-lattices.

We conclude that the ground-state of the system should be the one depicted in Fig. 2.

Notice it is an RVB-like state [9–11], where the resonating dimers, instead of being zero-total-spin pairs of localized Cu spins, are spin zero Cooper pairs formed out of two nearest neighbor holes belonging, each of them, to different sublattices A and B of the oxygen square lattice.

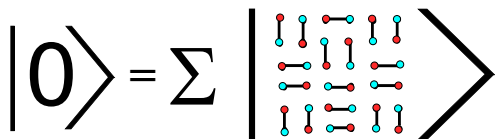


FIG. 2: The ground-state in the SC phase.

We are going to integrate out the ferromagnetic fluctuations by performing the quadratic functional integral on  $\mathbf{L}$ . This will produce three terms, corresponding to the square of the last term in (9): the 2nd term squared, which provides a kinetic term for  $\mathbf{n}$  [1], the 1st term squared, which produces an effective interaction among the itinerant doped holes (which is the 3rd term in the exponent of the expression below) and the crossed term, which vanishes [5, 13], yielding

### 2.3 Perturbation Theory in $H_0$

The complete effective Hamiltonian we use for describing the cuprates is obtained by carrying on a second order perturbation theory on the  $H_0 + H_U$  terms [1]. Including this result, we obtain the following effective Hamiltonian:

$$\begin{aligned}
H_{eff}[\psi] = & -t \sum_{\mathbf{R}, \mathbf{d}_i} \psi_{A\sigma}^\dagger(\mathbf{R}) \psi_{B\sigma}(\mathbf{R} + \mathbf{d}_i) + hc \\
& -g_S \sum_{\mathbf{R}, \mathbf{d}_i} \left[ \psi_{A\uparrow}^\dagger(\mathbf{R}) \psi_{B\downarrow}^\dagger(\mathbf{R} + \mathbf{d}_i) + \psi_{B\uparrow}^\dagger(\mathbf{R} + \mathbf{d}_i) \psi_{A\downarrow}^\dagger(\mathbf{R}) \right] \left[ \psi_{B\downarrow}(\mathbf{R} + \mathbf{d}_i) \psi_{A\uparrow}(\mathbf{R}) + \psi_{A\downarrow}(\mathbf{R}) \psi_{B\uparrow}(\mathbf{R} + \mathbf{d}_i) \right] \\
& -g_P \sum_{\mathbf{R}, \mathbf{d}_i} \left[ \psi_{A\uparrow}^\dagger(\mathbf{R}) \psi_{B\uparrow}(\mathbf{R} + \mathbf{d}_i) + \psi_{A\downarrow}^\dagger(\mathbf{R}) \psi_{B\downarrow}(\mathbf{R} + \mathbf{d}_i) \right] \left[ \psi_{B\uparrow}^\dagger(\mathbf{R} + \mathbf{d}_i) \psi_{A\uparrow}(\mathbf{R}) + \psi_{B\downarrow}^\dagger(\mathbf{R} + \mathbf{d}_i) \psi_{A\downarrow}(\mathbf{R}) \right], \quad (14)
\end{aligned}$$

where  $g_S$ , is the hole-attractive interaction coupling parameter and  $g_P$ , the hole-repulsive one, given, respectively, by

$$g_S = \frac{J_K^2}{8J_{AF}} \quad g_P = \frac{2t_p^2}{U_p} \quad (15)$$

This is the effective Hamiltonian of our theory for High-Tc cuprates.

## 2.4 The Effective Hamiltonian: Hubbard-Stratonovitch Fields

We can write our effective Hamiltonian in terms of the Hubbard-Stratonovitch fields  $\Phi$  and  $\chi$ , as [1]

$$\begin{aligned}
H_{eff} = & -t_p \sum_{\mathbf{R}, \mathbf{d}_i} \sum_{\sigma} \psi_{A,\sigma}^\dagger(\mathbf{R}) \psi_{B,\sigma}(\mathbf{R} + \mathbf{d}_i) + hc \\
& + \sum_{\mathbf{R}, \mathbf{d}_i} \Phi(\mathbf{R}, \mathbf{d}_i) \left[ \psi_{A\uparrow}^\dagger(\mathbf{R}) \psi_{B\downarrow}^\dagger(\mathbf{R} + \mathbf{d}_i) + \psi_{B\uparrow}^\dagger(\mathbf{R} + \mathbf{d}_i) \psi_{A\downarrow}^\dagger(\mathbf{R}) \right] + hc \\
& + \sum_{\mathbf{R}, \mathbf{d}_i} \chi(\mathbf{R}, \mathbf{d}_i) \left[ \psi_{A\uparrow}^\dagger(\mathbf{R}) \psi_{B\uparrow}(\mathbf{R} + \mathbf{d}_i) + \psi_{A\downarrow}^\dagger(\mathbf{R}) \psi_{B\downarrow}(\mathbf{R} + \mathbf{d}_i) \right] + hc \\
& + \frac{1}{g_S} \sum_{\mathbf{R}, \mathbf{d}_i} \Phi^\dagger(\mathbf{R}, \mathbf{d}_i) \Phi(\mathbf{R}, \mathbf{d}_i) + \frac{1}{g_P} \sum_{\mathbf{R}, \mathbf{d}_i \in \mathbf{R}} \chi^\dagger(\mathbf{R}, \mathbf{d}_i) \chi(\mathbf{R}, \mathbf{d}_i), \quad (16)
\end{aligned}$$

In order to describe the doping process, we add to the above Hamiltonian the chemical potential term

$$-\mu \left[ \sum_{\sigma} \left( \psi_{A,\sigma}^\dagger \psi_{A,\sigma} + \psi_{B,\sigma}^\dagger \psi_{B,\sigma} \right) - d(x) \right] \quad (17)$$

where  $d(x)$  is a function of the stoichiometric doping parameter  $x$ , to be determined self-consistently.

From this we derive the field equations

$$\begin{aligned}
\Phi^\dagger(\mathbf{R}, \mathbf{d}_i) = & \quad (18) \\
g_S \left[ \psi_{A\uparrow}^\dagger(\mathbf{R}) \psi_{B\downarrow}^\dagger(\mathbf{R} + \mathbf{d}_i) + \psi_{B\uparrow}^\dagger(\mathbf{R} + \mathbf{d}_i) \psi_{A\downarrow}^\dagger(\mathbf{R}) \right]
\end{aligned}$$

and

$$\begin{aligned}
\chi^\dagger(\mathbf{R}, \mathbf{d}_i) = & \quad (19) \\
g_P \left[ \psi_{A\uparrow}^\dagger(\mathbf{R}) \psi_{B\uparrow}(\mathbf{R} + \mathbf{d}_i) + \psi_{A\downarrow}^\dagger(\mathbf{R}) \psi_{B\downarrow}(\mathbf{R} + \mathbf{d}_i) \right]
\end{aligned}$$

Observe that  $\Phi^\dagger$  creates two holes with opposite spins, each one in neighboring sites). It is, therefore, a Cooper pair creation operator.  $\chi^\dagger$ , conversely, creates an electron and a hole with parallel spins, also in the neighboring sites  $A, B$ . It is, therefore, a spin one exciton creation operator.

Let us examine the ground-state expectation value of

these operators, namely

$$\Delta(\mathbf{d}_i) = g_S \left\langle \psi_{A\uparrow}^\dagger(\mathbf{R}) \psi_{B\downarrow}^\dagger(\mathbf{R} + \mathbf{d}_i) + \psi_{B\uparrow}^\dagger(\mathbf{R} + \mathbf{d}_i) \psi_{A\downarrow}^\dagger(\mathbf{R}) \right\rangle \quad (20)$$

and

$$M(\mathbf{d}_i) = g_P \left\langle \psi_{A\uparrow}^\dagger(\mathbf{R}) \psi_{B\uparrow}^\dagger(\mathbf{R} + \mathbf{d}_i) + \psi_{A\downarrow}^\dagger(\mathbf{R}) \psi_{B\downarrow}^\dagger(\mathbf{R} + \mathbf{d}_i) \right\rangle \quad (21)$$

Notice that, because of the invariance under Bravais lattice translations, it follows that  $\Delta(\mathbf{d}_i)$  and  $M(\mathbf{d}_i)$  do not depend on the Bravais lattice sites' position  $\mathbf{R}$ , rather, they depend only on  $\mathbf{d}_i$ .

We find [1], in momentum space

$$\Delta(\mathbf{k}) = \Delta [\cos k_+ a' - \cos k_- a'] \quad (22)$$

and also that

$$M(\mathbf{k}) = M [\cos k_+ a' - \cos k_- a'] \quad (23)$$

where  $k_\pm = \frac{k_x \pm k_y}{\sqrt{2}}$ .

We see that the SC and PG order parameters both have a d-wave symmetry, namely, change the sign under a 90° rotation, and have nodal lines along the  $\pm\hat{x}$  and  $\pm\hat{y}$  directions

### 3 THE PHASE DIAGRAM OF CUPRATES

#### 3.1 The Stationary Point

Replacing  $\Phi$  and  $\chi$  by their ground-state expectation values  $\Delta$  and  $M$  in the Hamiltonian (16), and using this in the grand-canonical ensemble, after functional integration over the fermionic (holes) degrees of freedom, we obtain the grand-canonical potential where

$$\Omega(\Delta, M, \mu) = -k_B T \ln Z_G(\Delta, M, \mu) \quad (24)$$

where

$$Z_G(\Delta, M, \mu) = \text{Tr}_\Psi e^{-\beta\{H - \mu\mathcal{N}\}} \quad (25)$$

is the grand-partition function.

Using the four-component Nambu fermion field,

$$\Psi_a = \begin{pmatrix} \psi_{A,\uparrow,a} \\ \psi_{B,\uparrow,a} \\ \psi_{A,\downarrow,a}^\dagger \\ \psi_{B,\downarrow,a}^\dagger \end{pmatrix}, \quad (26)$$

in which the index  $a$  indicates to which of the parallel  $\text{CuO}_2$  planes the electrons and holes belong and runs from 1 to  $N$ , where  $N = 1, 2, 3, \dots$ , according to the number of planes the specific material possesses.

In matrix form then

$$\mathcal{H} - \mu\mathcal{N} = \begin{pmatrix} -\mu & \epsilon + M & 0 & \Delta \\ \epsilon + M^* & -\mu & \Delta & 0 \\ 0 & \Delta^* & \mu & -\epsilon - M^* \\ \Delta^* & 0 & -\epsilon - M & \mu \end{pmatrix} \quad (27)$$

The corresponding eigenvalues of  $\mathcal{H} - \mu\mathcal{N}$ , are

$$\mathcal{E}_\pm(\mathbf{k}) = \sqrt{(\sqrt{\epsilon^2(\mathbf{k}) + |M(\mathbf{k})|^2} \pm \mu)^2 + |\Delta(\mathbf{k})|^2}. \quad (28)$$

Then, notice that  $\Delta$  and  $M$  in (27), effectively act as hopping parameters for the fermion field, similarly to the dimerization field in the Su-Schrieffer-Heeger model for polyacetylene [5, 12]. In that case, dimerization produces a nonzero ground-state expectation value of that field, which generates a gap for the electrons. In the case of the cuprates, the occurrence of nonzero values for  $\Delta$  and  $M$ , respectively, produce a SC gap and the pseudogap.

Also, from  $H_0$ , we obtain the tight-binding result

$$\epsilon(\mathbf{k}) = -2t [\cos k_+ a + \cos k_- a], \quad (29)$$

Using the eigenvalues  $\mathcal{E}_\pm(\mathbf{k})$ , given in (28), we can write

$$\Omega[\Delta, M, \mu] = \frac{|\Delta|^2}{g_S} + \frac{|M|^2}{g_P} + N\mu d(x) - 2NT \sum_{l=\pm 1} \left(\frac{a}{2\pi}\right)^2 \int d^2k \ln \cosh \{\mathcal{E}_l(\mathbf{k})\} \quad (30)$$

Minimizing the effective potential with respect to the three variables, we find the following three equations:

$$2\Delta_{\mathbf{k}} \left[ -\frac{2T}{\alpha} F(\Delta_{\mathbf{k}}, M_{\mathbf{k}}, \mu) + \frac{\eta(Ng_S)}{g_c} \right] = 0 \quad (31)$$

$$2M_{\mathbf{k}} \left[ -\frac{2T}{\alpha} F(\Delta_{\mathbf{k}}, M_{\mathbf{k}}, \mu) + \frac{\eta(Ng_P)}{g_c} \right] = 0 \quad (32)$$

and

$$d(x) = \mu \frac{4T}{\alpha} F(\Delta_{\mathbf{k}}, M_{\mathbf{k}}, \mu) \quad (33)$$

where  $F(\Delta_{\mathbf{k}}, M_{\mathbf{k}}, \mu)$  is a function, which, in the regime where  $|\Delta_0| \sim 0, |M_0| \sim 0$  is given by

$$F(\Delta_0, M_0, \mu_0)|_{|\Delta_0| \sim 0, |M_0| \sim 0} = \ln 2 + \frac{1}{2} \ln \cosh \left[ \frac{\sqrt{|\Delta_0|^2 + (|M_0| + \mu_0(x))^2}}{2T} \right] + \frac{1}{2} \ln \cosh \left[ \frac{\sqrt{|\Delta_0|^2 + (|M_0| - \mu_0(x))^2}}{2T} \right] \quad (34)$$

and

$$\eta(Ng) = \frac{Ng - g_c}{Ng} \quad ; \quad g_c = \frac{\alpha}{\Lambda} \quad (35)$$

$\eta(g)$  is a monotonically increasing function that saturates at infinity, namely

$$\eta(g) \xrightarrow{g \rightarrow \infty} 1. \quad (36)$$

In the expressions above,

$$\alpha = 2\pi \left[ \frac{\hbar v_{eff}}{a} \right]^2$$

, where  $\hbar v_{eff}$  is the characteristic velocity.

$\Lambda$  is a characteristic energy scale, which appears [13] in connection to the characteristic length of the system. A natural choice for the latter is the coherence length  $\xi$ , which essentially measures the range of the pairing interaction (or the Cooper pair size). In cuprates we have  $\xi \geq \xi_0 \simeq 10\text{\AA}$ , whereas in conventional superconductors  $\xi \geq \xi_0 \simeq 500\text{\AA}$ . The energy cutoff is then

$$\Lambda \simeq 2\pi \left[ \frac{\hbar v_{eff}}{\xi} \right]$$

. It determines the energy scale below which we may consider Cooper pairs as quasiparticles, hence it must be of the order of  $T_c$ .

We have

$$g_c = \frac{\alpha}{\Lambda} = \frac{\Lambda}{2\pi} \left[ \frac{\xi}{a} \right]^2. \quad (37)$$

The numerical values for LSCO would be  $a = 3.75 \text{\AA}$ ,  $\Lambda = 0.018 \text{ eV}$ ,  $g_c = 0.30 \text{ eV}$ ,  $\xi \simeq 38.6 \text{\AA}$ . The characteristic velocity would be given by  $\hbar v = 0.110 \pm 0.016 \text{ eV}\text{\AA}$ .

From (31), it follows that the critical temperature for the onset of superconductivity is given by

$$T_c(x) = \frac{\frac{\Lambda \eta(Ng_S)}{2}}{\ln 2 + \ln \cosh \frac{\mu_0(x)}{T_c(x)}} \quad (38)$$

Now, the denominator in the above expression is a monotonically increasing function of  $\mu_0$ , hence it follows that the maximum value of  $T_c$ , will occur for a  $x_0$  such that  $\mu_0(x_0) = 0$ . From this, we choose the simplest parametrization for the chemical potential  $\mu_0(x)$  along the transition curve  $T_c(x)$ , namely,

$$\mu_0(x) = 2\gamma(x_0 - x) \quad (39)$$

where  $\gamma$  is a parameter to be adjusted, which for LSCO turns out to be:  $\gamma = 0.020 \text{ eV}$ .

The optimal  $T_c$ , hence, is given by

$$T_c^{max} = \frac{\Lambda \eta(Ng_S)}{2 \ln 2} \quad (40)$$

In the table below, we show the optimal SC transition temperature obtained from this formula for several High-Tc cuprates and compare with the corresponding experimental values. The magnitudes of the  $g_S$  couplings are determined in [1, 4].

	N	$T_{max}^{th}(K)$	$T_{max}^{exp}(K)$
Bi2201	1	34.76	34.8
Bi2212	2	92.79	92.8
Bi2223	3	112.13	110
Hg1201	1	96.90	96.8
Hg1212	2	126.99	127
Hg1223	3	137.07	138
Tl2201	1	89.99	89
Tl2212	2	118.99	119
Tl2223	3	128.99	128

TABLE I: Comparison between the theoretical value of the optimal SC transition temperature, given by Eq. (40) with the corresponding experimental values [1, 4] for the Bi, Hg and Tl families of cuprates.

Considering the case of LSCO, for which  $T_c^{max} = 0.0031 \text{ eV}$ , using the equation above, we immediately find  $g_S = 0.39406$ . Now, inserting in (15) the values for the Kondo and Heisenberg couplings, derived from the Spin-Fermion system [14]:  $J_K = 1.17 \text{ eV}$  and  $J_{AF} = 0.43 \text{ eV}$ , we obtain

$$\frac{J_K^2}{8J_{AF}} = 0.39793 \quad (41)$$

which is remarkably close to the experimentally determined value:  $g_S = 0.39406$

The pseudogap transition temperature  $T^*$  can be obtained from (32), namely

$$T^*(x) = \frac{\frac{\Lambda \eta(Ng_P)}{2}}{\ln \left[ 1 + \exp \left[ -\frac{\mu_0(x)}{T^*(x)} \right] \right]} \quad (42)$$

where we chose the parametrization

$$\tilde{\mu}_0(x) = 2\tilde{\gamma}(\tilde{x}_0 - x) \quad (43)$$

for the chemical potential along the pseudogap transition line  $T^*(x)$ .  $\tilde{\gamma}$  is the only adjustable parameter, which for LSCO results in  $\tilde{\gamma} = 0.180 \text{ eV}$ .

As it turns out, the following identity holds [4] (Supplementary Material):

$$\gamma x_0 \eta(N=1)^{1/N} = \tilde{\gamma} \tilde{x}_0 \tilde{\eta}(N=1)^{1/N}. \quad (44)$$

From this equation, we determine  $\tilde{\eta}(1) \equiv \eta(g_P) = 0.01565$ , and out of which we obtain  $g_P = 0.30476 \text{ eV}$ .

Now, using in (15) the values for the hopping and Hubbard parameters, derived from the Spin-Fermion system, namely, [14]:  $t = 0.91$  eV and  $U = 5.50$  eV, we obtain

$$\frac{2t^2}{U} = 0.30113 \text{ eV} \quad (45)$$

which is remarkably close to the experimentally determined value:  $g_P = 0.30476$  eV.

From (38), we can derive [1]

$$\begin{cases} T_c(x) = \frac{\ln 2 \ T_{max}}{\ln 2 + \frac{\mu_0(x)}{2T_c(x)} - \frac{1}{2} \left(1 - e^{-\frac{\mu(x)}{T_c(x)}}\right)}, & x < x_0 \\ T_c(x) = \frac{\ln 2 \ T_{max}}{\ln \left[1 + \exp\left[-\frac{\mu(x)}{T_c(x)}\right]\right]}, & x > x_0 \end{cases} \quad (46)$$

the application of which to Hg1201, we display in Fig.3. For this compound, we find  $\gamma = 0.031$  eV and  $\tilde{\gamma} = 0.186$  eV

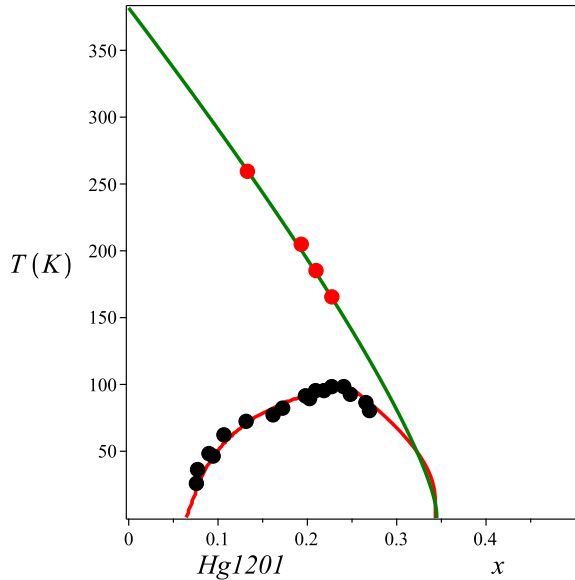


FIG. 3: The phase diagram of Hg1201, showing the SC and PG phases. The solid lines correspond to analytical expressions derived from our theory, namely, (42) and (46) [1]. Experimental data from [21].

## 4 THE RESISTIVITY OF HIGH-TC CUPRATES

### 4.1 General expression for $\rho(T, x)$

Let us determine the resistivity as a function of the temperature in the different non-SC phases of cuprates.

For this purpose, we shall use the Kubo formula for the conductivity at a finite temperature [15] and invert it. The DC conductivity matrix is given by

$$\sigma_{\text{DC}}^{ij} = \lim_{\omega \rightarrow 0} \frac{i}{\omega} [1 - e^{-\beta\hbar\omega}] \lim_{\mathbf{k} \rightarrow \mathbf{0}} \Pi^{ij}(\omega + i\delta, \mathbf{k}), \quad (47)$$

where  $\Pi^{ij}$  is the retarded, connected current-current correlation function:

$$\Pi^{ij} = \langle j^i j^j \rangle_C, \quad (48)$$

which is given by

$$\langle j^i j^j \rangle_C(\omega, \mathbf{k}) = \frac{\delta^2 \Omega[\mathbf{A}]}{\delta \mathbf{A}^i(\omega, \mathbf{k}) \delta \mathbf{A}^j(\omega, \mathbf{k})}, \quad (49)$$

where  $\Omega[\mathbf{A}]$  is the grand-canonical potential in the presence of an applied electromagnetic vector potential  $\mathbf{A}(\omega, \mathbf{k})$  that is obtained from

$$Z[\mathbf{A}] = \text{Tr}_{\text{Total}} e^{-\beta[H[\mathbf{A}] - \mu N]}. \quad (50)$$

The electromagnetic field  $\mathbf{A}$  is introduced through the usual minimal coupling prescription

$$\epsilon(\hbar\mathbf{k}) \longrightarrow \epsilon(\hbar\mathbf{k} + e\mathbf{A}), \quad (51)$$

which yields the grand-canonical potential in the presence of an applied electromagnetic vector potential  $\mathbf{A}$ , namely,  $\Omega[\mathbf{A}]$ .

Using (49), and (51), we obtain

$$\langle j^i j^j \rangle(\mathbf{k} = 0, \omega = 0) = N \sum_{l=\pm 1} \frac{\partial^2 \mathcal{E}_l[\mathbf{A}]}{\partial \mathbf{A}^i \partial \mathbf{A}^j} \tanh\left(\frac{\mathcal{E}_l[\mathbf{A}]}{2k_B T}\right). \quad (52)$$

where

$$\mathcal{E}_l^2[\mathbf{A}] = \Delta_0^2 + \left(\sqrt{v^2(\hbar\mathbf{k} + e\mathbf{A})^2 + M^2} + l\mu\right)^2. \quad (53)$$

Inserting the last expression in (52) and this in (47) we obtain the DC conductivity per  $\text{CuO}_2$  plane, after inverting the conductivity matrix and dividing by  $N$  [2]:

$$\rho^{ij} = \left( \frac{\sigma_{\text{DC}}^{ij}}{N} \right)^{-1} = \frac{\delta^{ij} M}{\hbar\beta V^{-1} e^2 v^2 \left\{ \frac{|M+\mu|}{\sqrt{\Delta^2 + (M+\mu)^2}} \tanh \left[ \frac{\sqrt{\Delta^2 + (M+\mu)^2}}{2k_B T} \right] + \frac{|M-\mu|}{\sqrt{\Delta^2 + (M-\mu)^2}} \tanh \left[ \frac{\sqrt{\Delta^2 + (M-\mu)^2}}{2k_B T} \right] \right\}}. \quad (54)$$

where  $V = da^2$  is the volume of the primitive unit cell, per  $\text{CuO}_2$  plane, with  $d$  being the distance between planes,  $a$  the lattice parameter and  $v$ , the characteristic velocity of the holes, such that  $(\hbar v/a) \approx 2.86 \times 10^{-2} eV$  [2].

In the SC phase, we have  $\Delta \neq 0$  and  $M = 0$ , implying that the resistivity vanishes as it should:

$$\rho_{\text{SC}}^{ij} = \frac{\delta^{ij} M}{\hbar\beta V^{-1} e^2 v^2 \left\{ \frac{2|\mu|}{\sqrt{\Delta^2 + \mu^2}} \tanh \left[ \frac{\sqrt{\Delta^2 + \mu^2}}{2k_B T} \right] \right\}} \xrightarrow{M \rightarrow 0} 0 \quad (55)$$

In the non-superconducting phases, conversely, we have  $\Delta = 0$ , which leads to the following expression for the resistivity

$$\rho^{ij} = \frac{\delta^{ij} M}{\hbar\beta V^{-1} e^2 v^2 \left\{ \tanh \left[ \frac{M+\mu}{2k_B T} \right] + \tanh \left[ \frac{M-\mu}{2k_B T} \right] \right\}}. \quad (56)$$

This can be rewritten as

(From now on we will drop the  $ij$  index)

$$\rho(x, T) = BT^2 G \left( \frac{M}{k_B T}, \frac{\mu}{k_B T} \right), \quad (57)$$

where the scaling function  $G$  of the critical variables  $K_1 = M_0/k_B T$  and  $K_2 = \mu/k_B T$ , given by

$$G(K_1, K_2) = K_1 \frac{\cosh K_1 + \cosh K_2}{2 \sinh(K_1)}, \quad (58)$$

In the previous expressions the (almost universal) constant  $B$  is

$$B = \frac{\hbar}{e^2} \frac{d}{2\pi} \left( \frac{a}{\hbar v} \right)^2 k_B^2 \approx 0.37 \times d \text{ n}\Omega\text{cm}/K^2, \quad (59)$$

where  $\hbar/e^2 \approx 25812.807\Omega$  is the resistance quantum and  $d$  is given in  $\text{\AA}$  -units.

This general form of the resistivity, whose dependence on the temperature ( $T$ ) and on the doping parameter ( $x$ ) has been made explicit, holds in all phases of the phase diagram of cuprates, except the SC one. The peculiar form of the resistivity in each of the different phases will be determined by the form the function  $G(K_1, K_2)$  assumes in each phase.

## 4.2 The Resistivity in each Phase

The scaling function, in the different non-SC phases of cuprates [2]

$$G(K_1, K_2) = \begin{cases} \exp[K_2 - K_1] & K_1 \neq 0; K_2 \neq 0; \text{PG} \\ C \frac{T^*}{T} & K_1 = 0; K_2 \neq 0; \text{SM} \\ 1 & K_1 = 0; K_2 = 0; \text{FL} \end{cases} \quad (60)$$

The results above immediately imply a  $T^2$  dependence of the resistivity in the FL phase, with a coefficient  $B \simeq 2.45 \text{ n}\Omega\text{cm}/K^2$ , which remarkably agrees with the

experimental result [17]  $B \simeq 2.50 \pm 0.1 \text{ n}\Omega\text{cm}/K^2$ .

$$\rho_{\text{FL}}(T) = BT^2 \quad (61)$$

It also implies the resistivity has a linear dependence

on  $T$  with a slope proportional to  $T^*$  in the SM phase.

$$\rho_{SM}(T) = BCT^*T \quad (62)$$

where  $C = \cosh\left(\frac{D}{2}\right)$  and  $K_2 = D$ .

In the PG phase, conversely, the resistivity presents an exponential dependence on  $T$  for  $K_2 > K_1$ , a quadratic dependence on  $T$ , for  $K_2 \approx K_1$  and a linear dependence on  $T$  for  $K_1 \rightarrow 0$ , namely,

$$\rho_{PG}(T) \propto \begin{cases} T^2 e^{1/T} & K_2 > K_1 \\ T^2 & K_2 \simeq K_1 \\ T & K_1 \rightarrow 0 \end{cases} \quad (63)$$

## 5 THE INFLUENCE OF AN APPLIED PRESSURE ON THE SC TEMPERATURE $T_c(x)$

We have seen in [1] that, under an applied pressure  $P$ , the SC coupling varies as

$$g_S(P) = g_S e^{P/\kappa}, \quad (64)$$

where  $\kappa$  must be adjusted. Hereafter, we use the convention that  $P$  is the pressure with respect to the atmospheric pressure:  $P = P_T - P_{atm}$ , where  $P_T$  is the total pressure.

The function  $\eta(g_S)$ , consequently, changes as

$$\eta(P) = 1 - \frac{g_c}{Ng_S(P)} \quad (65)$$

The optimal SC transition temperature,  $T_c(x = x_0; P)$ , by its turn, will be modified as

$$T_c(x_0; P) = \frac{\frac{\Delta\eta(P)}{2}}{\ln 2 + \frac{\gamma(P)x_0(P)\left[1 - \frac{x_0(0)}{x_0(P)}\right]}{T_c(x_0; P)} - \frac{1}{2} \left[ 1 - e^{-\frac{2\gamma(P)x_0(P)\left[1 - \frac{x_0(0)}{x_0(P)}\right]}{T_c(x_0; P)}} \right]}, \quad (66)$$

Now, from (44), it follows that

$$\begin{aligned} \gamma(P)x_0(P)\eta(N=1; P)^{1/N} &= \gamma(0)x_0(0)\eta(N=1; 0)^{1/N} \\ \gamma(P)x_0(P) &= \gamma(0)x_0(0) \frac{\eta(N=1; 0)^{1/N}}{\eta(N=1; P)^{1/N}}, \end{aligned} \quad (67)$$

Writing

$$\gamma(P) = \gamma(0)f(P) \quad ; \quad x_0(P) = x_0(0)g(P) \quad (68)$$

then, we have

$$f(P)g(P) = \frac{\eta(N=1; 0)^{1/N}}{\eta(N=1; P)^{1/N}} \equiv A(P) \quad (69)$$

Choosing  $g(P) = A^{1/2}(P)$ , we have  $f(P) = A^{1/2}(P)$ . Inserting in (66), we get

$$T_c(x_0; P) = \frac{\frac{\Delta\eta(P)}{2}}{\ln 2 + \frac{\gamma(0)x_0(0)[A(P) - A^{1/2}(P)]}{T_c(x_0; P)} - \frac{1}{2} \left[ 1 - e^{-\frac{2\gamma(0)x_0(0)[A(P) - A^{1/2}(P)]}{T_c(x_0; P)}} \right]}, \quad (70)$$

where  $\eta(P)$  is given by (65).

Now, solving for  $T_c(x_0, P)$ , assuming that  $x_0(P=0) = x_0$ , namely, that the system without pressure is at optimal doping, we obtain, for Hg1212 and Hg1223, using the parameters of Table 1 and adjusting in (64) only  $\kappa = 9 \text{ GPa}$  for the former and  $\kappa = 4 \text{ GPa}$  for the latter:

Notice that for  $P = 0$ , our expression (70) reduces to the optimal temperature (40).

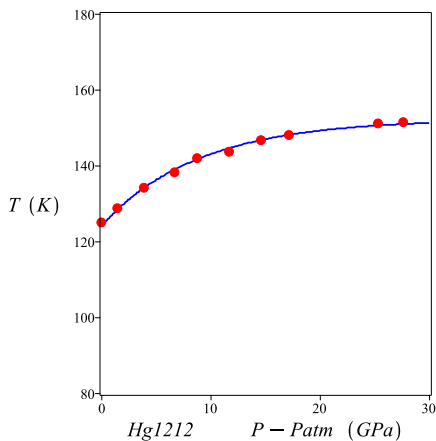


FIG. 4:  $T_c(x = x_0(0); P)$  for Hg1212. The solid line is given by our analytical expression (70) by adjusting a single parameter, namely,  $\kappa = 9$  GPa. The experimental data are from [18]

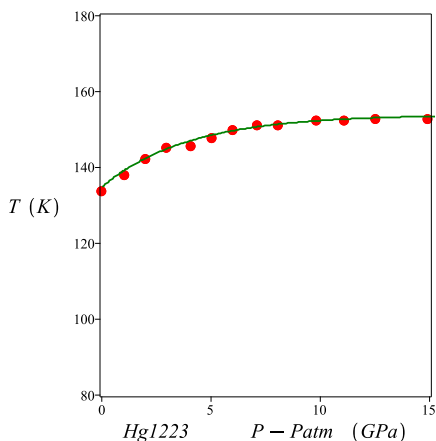


FIG. 5:  $T_c(x = x_0(0); P)$  for Hg1223. The solid line is given by our analytical expression (70) by adjusting a single parameter, namely,  $\kappa = 4$  GPa. The experimental data are from [18]

## 6 CONCLUSION

In summary, we have described the main features and some of the main applications of a theory for the superconductivity in cuprates that we have developed recently. This theory has allowed for the obtainment of the theoretical values of several observables that are relevant for the cuprates, which agree quite well with the corresponding experimentally measured values.

The pairing mechanism in our theory derives from the ferromagnetic fluctuations of the Kondo-like interaction that exists between the oxygen doped holes and the localized Cu ions. After a dimerization that occurs in the oxygen lattice, the mutual interaction of the holes with the Cu ions, produces a net attraction between neighboring holes, which leads to a superconducting RVB-like

state in which the resonating dimers are Cooper pairs [4]. The AF magnetically ordered phase derives from the antiferromagnetic fluctuations of the holes-Cu ions interaction.

The Pseudogap, conversely, stems from the Coulomb repulsion among the oxygen holes or, equivalently, the Coulomb attraction between electrons and holes in the oxygen atoms. The main mechanism responsible for the resistivity in the normal phases consists of hole-exciton scattering. This naturally leads to a T-linear resistivity. The PG  $T^*(x)$  line characterizes a continuous transition, whose order parameter is the ground-state expectation value of the exciton creation operator. The PG phase is an exciton condensate,  $M \neq 0$ .  $M$  and  $\Delta$  compete: they cannot be both nonzero in the same phase. We are presently working on the description of the charge-ordered phase that opens within the Pseudogap phase, as well as on the theoretical description of the Neel phase and transition temperature  $T_N$ .

## Acknowledgements

The author is grateful to Nigel Hussey and Jake Ayres for interesting and stimulating conversations. This study received partial financial support from CNPq, FAPERJ and CAPES.

---

\* marino@if.ufrj.br

- [1] E. C. Marino, R. O. Corrêa Jr, R. Arouca, L. H. C. M. Nunes, and V. S. Alves, *Superconducting and Pseudogap Transition Temperatures in High-Tc Cuprates and the Tc Dependence on Pressure*, Supercond. Sci. and Tech. 33, 035009 (2020)
- [2] R. Arouca and E. C. Marino, *The resistivity of High-Tc Cuprates*, Supercond. Sci. and Tech. 34, 035004 (2021)
- [3] E. C. Marino and R. Arouca, *Magnetic Field Effect on the transport properties of high-Tc Cuprates*, Supercond. Sci. and Tech. 34, 085008 (2021)
- [4] E. C. Marino, *Three Studies in High-Tc Cuprates*, New J. of Phys. 24, 063009 (2022)
- [5] E. C. Marino, *Quantum Field Theory Approach to Condensed Matter Physics*, Cambridge University Press, Cambridge, UK (2017)
- [6] J. Zaanen and A. M. Oleś, *Canonical perturbation theory and the two-band model for high-T<sub>c</sub> superconductors*, Phys. Rev. B 37, 9423 (1988)
- [7] E. C. Marino and M. B. S. Neto, *Magnetic-texture-driven charge pairing in the spin-fermion Hubbard model and superconductivity in the high-T<sub>c</sub> cuprates*, Phys. Rev. B 66, 224512 (2002).
- [8] E. C. Marino and M. B. S. Neto, *Quantum skyrmions and the destruction of long-range antiferromagnetic order in the high-T<sub>c</sub> superconductors LSCO and YBCO*, Phys. Rev. B 64, 092511 (2001).
- [9] P. W. Anderson, *Resonating valence bonds: A new kind of insulator?*, Materials Research Bulletin 8, 153 (1973); P. Fazekas and P. W. Anderson, *On the ground state properties of the anisotropic triangular antiferromagnet*, Philosophical Magazine 30, 423 (1974).
- [10] P. W. Anderson, *The resonating valence bond state in La<sub>2</sub>CuO<sub>4</sub> and superconductivity*, Science 235, 1196 (1987).
- [11] B. Edegger, V. N. Muthukumar and C. Gros, *Gutzwiller-RVB theory of high-temperature superconductivity: Results from renormalized mean-field theory and variational Monte Carlo calculations*, Advances in Physics 56, 927 (2007).
- [12] W. Su, J. R. Schrieffer and A. J. Heeger, *Solitons in polyacetylene*, Phys. Rev. Letters 42, 1698 (1979).
- [13] E. C. Marino and L. H. C. M. Nunes, *Quantum criticality and superconductivity in quasi-two-dimensional Dirac electronic systems*, Nucl. Phys. B 741, 404 (2006).
- [14] P. Hansmann, N. Parragh, A. Toschi, G. Sangiovanni, and K. Held, *Importance of d-p Coulomb interaction for high T<sub>c</sub> cuprates and other oxides*, New. J. Phys. 16, 033009 (2014)
- [15] G. D. Mahan, *Many-Particle Physics*, Springer Science Business Media, (2013).
- [16] O. Cyr-Choinière, R. Daou, F. Laliberté, C. Collignon, S. Badoux, D. LeBoeuf, J. Chang, B. J. Ramshaw, D. A. Bonn, W. N. Hardy, R. Liang, J.-Q. Yan, J.-G. Cheng, J.-S. Zhou, J. B. Goodenough, S. Pyon, T. Takayama, H. Takagi, N. Doiron-Leyraud, and Louis Taillefer *Pseudogap temperature T\* of cuprate superconductors from the Nernst effect*, Phys. Rev. B 97, 064502 (2018).
- [17] S. Nakamae, K. Behnia, N. Mangkorntong, M. Nohara, H. Takagi, S. J. C. Yates, and N. E. Hussey, Phys. Rev. B 68, 100502 (2003)
- [18] L. Gao, F. Chen, R. L. Meng, Y. Y. Xue and C. W. Chu, *Superconductivity up to 147 K in HgBa<sub>2</sub>CaCu<sub>2</sub>O<sub>6+δ</sub> under quasi-hydrostatic pressure*, Phil. Mag. Lett. 68 345 (1993)
- [19] S. Shimizu, S. Tabata, H. Mukuda, Y. Kitaoka, P. M. Shirage, H. Kito, and A. Iyo, *Antiferromagnetism, superconductivity, and pseudogap in three-layered high-T<sub>c</sub> cuprates Ba<sub>2</sub>Ca<sub>2</sub>Cu<sub>3</sub>O<sub>6</sub>(F, O)<sub>2</sub> probed by Cu-NMR*, Phys. Rev. B 83, 214514 (2011)
- [20] O. Cyr-Choinière, R. Daou, F. Laliberté, C. Collignon, S. Badoux, D. LeBoeuf, J. Chang, B. J. Ramshaw, D. A. Bonn, W. N. Hardy, R. Liang, J.-Q. Yan, J.-G. Cheng, J.-S. Zhou, J. B. Goodenough, S. Pyon, T. Takayama, H. Takagi, N. Doiron-Leyraud, and L. Taillefer, *Pseudogap temperature T\* of cuprate superconductors from the Nernst effect*, Phys. Rev. B 97, 064502 (2018)
- [21] A. Yamamoto, W.-Z. Hu and S. Tajima, *Thermoelectric power and resistivity of HgBa<sub>2</sub>CuO<sub>4+δ</sub> over a wide doping range*, Phys. Rev. B 63, 024504 (2000)  
*La<sub>(2-x)Sr<sub>x</sub>CuO<sub>4</sub></sub>*